Optics Communications 282 (2009) 1961–1968

Contents lists available at ScienceDirect

Optics Communications

journal homepage: www.elsevier.com/locate/optcom

Novel accurate computer algorithm for modeling light propagation and diffraction in inhomogeneous, anisotropic medium – Applied to the acousto-optic interaction

Gábor Mihajlik *, Pál Maák, Attila Barócsi, Péter Richter

Technical University of Budapest, Department of Atomic Physics, Budafoki ut8, H-1111 Budapest, Hungary

ARTICLE INFO

Article history:
Received 28 August 2008
Received in revised form 8 January 2009
Accepted 2 February 2009

PACS:
42.79.Jq
85.60.Bt

Keywords:
Vectorial light propagation in anisotropic
Inhomogeneous medium
Computational model
Optical anisotropy
Acousto-optic interaction

ABSTRACT

There is a high demand for a computational model that calculates effectively the phase and amplitude distribution of the beams emerging from an acousto-optic cell. We present a model based on a new algorithm that is capable to solve the vectorial optical wave equation on consecutive planes in an optically anisotropic medium with an arbitrary refractive index distribution with limited refractive index amplitude. Strength of the presented method is that it does not require the paraxial approximation. We used the model successfully to calculate the amplitude and phase distribution of the diffracted and undiffracted beams generated in optically anisotropic and isotropic acousto-optic interaction.

1. Introduction

There are many physical situations requiring the calculation of vectorial wave propagation in media where the refractive indices (or the parameters of the wave equation) are spatially varying and the variance is relatively small.

During the last decades a large number of papers and books were published dealing with the theory, principals and applications of light propagation. The complexity and accuracy of calculations evolve parallelly with the increase of computer speed and capacity. Analytical formulae [1–3] are deduced mainly for special cases, paraxial propagation along particular axes [1] or non-paraxial beams in isotropic [2] or homogeneous [3] background. Parallel to analytical formulae several numerical computational models were developed, some of them calculating scalar diffraction in the context of acousto-optic interaction [4–11], but nowadays many papers discuss vectorial diffraction related to various propagation and scattering problems [12–16]. Vectorial calculations are mostly restricted to homogeneous media [12,13], perturbed but isotropic media [14] or homogeneous scatterers embedded in homogeneous backgrounds [15,16]. An important question of the usability of these methods is the convergence, if the diffraction efficiency generated by the spatial refractive index variation is high.

Modeling of the acousto-optic effect also belongs to this problem area. The original model of Van Cittert (see for instance Ref. [4]) comprehends the acoustic wave as a series of consecutive phase gratings and applies the analytic formula of the phase grating (where the amplitudes of the diffraction orders are described by Bessel functions). There is something similar physical concept behind the adaptation of the well known split-step method [7–11] in the acousto-optic diffraction, where the phase grating is conceived as small perturbation of the field's phase. Originally in this method the influence of the phase grating onto the propagation itself is neglected. To our best knowledge, these methods use also scalar field calculation and were elaborated for isotropic interactions where the propagating zeroth and higher order diffracted beams are of the same polarization. In many reports about propagation and acousto-optic diffraction in anisotropic media paraxial approximation is used [1,3,7], because it allows simplification of the algorithm and reduces calculation time. However, some practical cases do not fulfill the paraxial requirements, like strongly focused beams – e.g. acousto-optic modulators – or cases where all

* Corresponding author. Tel.: +36 1 4634203.
E-mail address: mihajlikg@gmail.com (G. Mihajlik).

0030-4018/$ - see front matter © 2009 Published by Elsevier B.V.
doi:10.1016/j.optcom.2009.02.005

diffracted beams are treated as a common electric field distribution. The need for non-paraxial approximation in the case of large angle Bragg diffraction has been also shown numerically [9]. Vectorial representation of the electromagnetic field is needed to describe anisotropic propagation and diffraction in many practical acousto-optic devices [4,5]; however, we did not find comprehensive and general vectorial calculation of the anisotropic acousto-optic interaction where the polarization of the diffracted beams rotates during diffraction. Most of today's acousto-optic deflectors and filters use this anisotropic interaction characteristic to uniaxial crystals like TeO_2, $CaMoO_4$, $PbMoO_4$, etc. These devices are operating either in the Bragg regime (Klein–Cook parameter $Q \gg 1$), or at its limit ($Q \sim 1$) therefore our interest was focused onto this regime, where, with some limitations, practically only two diffraction orders, the zeroth and first are of importance. The anisotropic interaction is favored in these crystals, because of its high figure of merit and bandwidth. Here the first order diffracted optical beam is differently polarized than the zeroth order and the incident beam, therefore the model must handle electromagnetic field vectors.

We developed a general formalism able to handle vectorial beam propagation in acoustically perturbed background with high accuracy where the refractive index is anisotropic (or isotropic). The variance of the refractive index may be also general providing that the variance is relatively small. It may be a regular one like that caused by acoustic waves but it is not restricted only to sinusoidal refractive index distributions [4,5] it may be also irregular one, generated e.g. by thermal effects [6].

Though accuracy depends on the amount of afforded computational operations, our model does not require huge capacities of networks or supercomputers to obtain reasonable and practically far acceptable accuracy. The model does not utilize paraxial approximations, the approach is based on the integration of the complex wave equation along properly selected spatial directions.

The only restriction that we assumed is that reflecting beams are negligible which is true in the most cases. In some situations this condition is not fulfilled but it can be checked either experimentally or by calculation.

In connection with the acousto-optical methods mentioned above, it is important to underline that our method is substantially different from those based on successive diffraction, since it does not just add the modulated phase to the field in these intermediate planes but creates a perturbation approach that acts on the full field vector (amplitude, phase, polarization) as well as on the propagation between consecutive planes.

While our intention was primarily to model the Bragg regime and its limit nonetheless the presented method is not restricted to the Bragg regime, other diffraction orders are also well reproduced without additional effort if the Q parameter is lowered.

Section 2 contains the deduction of our model from the vectorial wave equation valid for anisotropic medium. Firstly we discuss the relations between accuracy and boundary conditions, then we deduce the anisotropic light propagation algorithm for homogeneous medium, and finally we extend it to inhomogeneous media.

We compare our computational results with physical expectations in Section 3 and conclude our work in Section 4.

2. Formalism

2.1. Boundary conditions and accuracy

Our goal was to calculate the most accurate solution of the electromagnetic wave equation for the case of light propagating in anisotropic and inhomogeneous medium (mainly conditions characteristic to the anisotropic acousto-optic interaction).

Using monochromatic light source we restrict the temporal variation of the field to the $\exp(-i\omega t)$ time dependence. For this case the Maxwell's equations result in the following complex wave equation:

$$\underline{\nabla} \times \underline{\nabla} \times \underline{E} - k_0^2 \underline{\underline{\varepsilon}}(\underline{r})\underline{E} = 0, \tag{1}$$

where $k_0 = \omega/c$ is the vacuum wave number, and the dielectric tensor

$$\underline{\underline{\varepsilon}}(\underline{r}) = \underline{\underline{\varepsilon_B}} + \underline{\underline{\Delta\varepsilon}}(\underline{r}) \quad \text{and} \quad \underline{\underline{\Delta\varepsilon}}(\underline{r}) \ll \underline{\underline{\varepsilon_B}}.$$

The inhomogeneous nature of the background is represented in the $\underline{\underline{\Delta\varepsilon}}(\underline{r})$ tensor which is a regular or irregular function of the space coordinate r. In the case of acousto-optic interaction this modulation is caused by the acoustic wave via the photoelastic effect and thermal effects [6].

Nevertheless, it is well known that certain solving methods cannot be carried out directly. For example the time-integration of the Maxwell's equations in the entire volume is not solvable, but because of the linearity it is even not necessary. In the case when the steady state light distribution corresponds to a monochromatic wave, the wave equation (1) – which is a second order partial differential equation – can be integrated along a spatial direction that must be properly selected. We call this special axis and the coordinate along it as z. The x and y axes are chosen perpendicular to the z axis to form a Euclidean coordinate system, and they can be freely chosen in the plane perpendicular to z.

The electric field and its partial derivate by z are known in a given plane perpendicular to z, at $z = 0$: $\underline{E}(x,y,0)$ and $\partial/\partial z\underline{E}(x,y,0)$, and from these, the electric field and its spatial derivatives can be determined with (1) in a parallel adjacent plane at a distance d from the source plane: $\underline{E}(x,y,d)$ and $\partial/\partial z\underline{E}(x,y,d)$. The problem is solvable when we introduce the assumption that d is infinitesimally small.

Nevertheless, beside its accuracy, this direct method also has a disadvantage: high technical requirements and computational time. Therefore it is useful to find an algorithm, which reduces computational time, but preserves accuracy.

We search an $\underline{E}(x,y,z)$ function, which satisfies the boundary conditions set by $\underline{E}(x,y,0)$, $\partial/\partial z\underline{E}(x,y,0)$, and also wave equation (1) with the approximation that the coordinate z is little. Substituting d into z: $\underline{E}(x,y,z)|_{z=d}$, can be perceived as a subsequent boundary condition for the next step.

The $\underline{E}(x,y,0)$ boundary condition and (1) can be satisfied by a wave $\underline{E}_+(x,y,z)$ propagating forward (towards increasing z) and by another wave $\underline{E}_-(x,y,z)$ propagating backward (towards decreasing z) and also by their linear combination. For example a forward propagating plane wave is described by $\exp(i \cdot k_+ \cdot r)$ and that of the backward propagating counterpart by $\exp(i \cdot k_- \cdot r)$, where $k_{+z} < 0$ and $k_{-z} > 0$.

Uniqueness of the complete solution is ensured by the $\partial/\partial z\underline{E}(x,y,0)$ boundary condition. This term provides the ratio of the backward and forward propagating beams. (If there is no backward propagating beam then the field is completely described by $\underline{E}(x,y,0)$).

Since in the practical cases that we intend to model reflecting beams are not measurable, we do not use the $\partial/\partial z\underline{E}(x,y,0)$ boundary condition for fitting, and so the backward propagating beams are completely neglected.

The partial differentials are calculated by Fourier transform. The experiences give the theoretically expected effect, that above a certain sampling frequency the results do not change (Sampling Theorem) which provides high accuracy without high computational need.

2.2. Propagation through homogeneous and anisotropic medium

If the medium is homogeneous, anisotropic ($\underline{\underline{\Delta\varepsilon}}(\underline{r}) = 0$), then the $\underline{E}(x,y,z)$ can be calculated from $\underline{E}(x,y,0)$ using Fourier transform for arbitrary z. In this case the wave equation simplifies to

$$\underline{\nabla} \times \underline{\nabla} \times \underline{E} - k_0^2 \underline{\underline{\varepsilon_B}} \underline{E} = 0. \tag{2}$$

The Fourier transform represents mathematically the decomposition of the beam into plane waves. The field vector of a plane wave characterized by the wave vector k is depending on the spatial position vector r as $\underline{E}_k(\underline{r}) = \underline{\tilde{E}} \exp(i\underline{kr})$. The corresponding equation holds for each particular plane wave component

$$\underline{k} \times (\underline{k} \times \underline{\tilde{E}}) - k_0^2 \underline{\underline{\varepsilon_B}} \underline{\tilde{E}} = 0.$$

From this equation two values for k_z can be obtained as a function of k_x and k_y, depending on the direction of $\underline{\tilde{E}}$. The amplitude vector $\underline{\tilde{E}}$ can be decomposed into ordinary and extraordinary components whose propagation is governed by these two k_z values. (The ordinary is denoted by subscript 'o', the extraordinary by 'e'.)

Similarly, the full field can be split to extraordinary and ordinary components also

$$\begin{aligned}\underline{E}(x,y,z) = &\iint \underline{\tilde{E}}_o(k_x,k_y) \cdot \exp[i(k_x x + k_y y)] \cdot \exp[i \cdot k_{oz}(k_x,k_y) \cdot z] \\ &\cdot \frac{dk_x dk_y}{4\pi} + \iint \underline{\tilde{E}}_e(k_x,k_y) \cdot \exp[i(k_x x + k_y y)] \\ &\cdot \exp[i \cdot k_{ez}(k_x,k_y) \cdot z] \cdot \frac{dk_x dk_y}{4\pi}\end{aligned} \tag{3}$$

To deduce $\underline{\tilde{E}}_o(k_x,k_y)$ and $\underline{\tilde{E}}_e(k_x,k_y)$ we take the Fourier transform of $E(x,y,0)$: $\underline{\tilde{E}}(k_x,k_y) = (x,y,0)\exp(-i(k_x x + k_y y))dx \cdot dy$. The polarization unit vectors are denoted by $\underline{e}_o(k_x,k_y)$ and $\underline{e}_e(k_x,k_y)$, for the ordinary and extraordinary polarizations, respectively. Using these unit vectors the plane wave amplitudes are represented by the decomposition: $\underline{\tilde{E}}(k_x,k_y) = \underline{\tilde{E}}_o + \underline{\tilde{E}}_e := \tilde{E}_o \cdot \underline{e}_o + \tilde{E}_e \cdot \underline{e}_e$. According to this the ordinary and extraordinary components can be directly calculated from the x, y components

$$\begin{bmatrix} \tilde{E}_o(k_x,k_y) \\ \tilde{E}_e(k_x,k_y) \end{bmatrix} = \begin{bmatrix} e_{o,x}(k_x,k_y) & e_{e,x}(k_x,k_y) \\ e_{o,y}(k_x,k_y) & e_{e,y}(k_x,k_y) \end{bmatrix}^{-1} \begin{bmatrix} \tilde{E}_x(k_x,k_y) \\ \tilde{E}_y(k_x,k_y) \end{bmatrix}$$

2.3. Light propagation through inhomogeneous and anisotropic medium

Here we discuss the case when the medium is inhomogeneous and anisotropic ($\underline{\underline{\Delta\varepsilon}}(\underline{r}) \neq 0$). The solution of the wave equation for the homogeneous medium is denoted by E_h, given by (3). The same for the inhomogeneous medium (perturbed with $\underline{\underline{\Delta\varepsilon}}(\underline{r})$) is E, and their difference is denoted by E_i

$$\underline{E} = \underline{E}_h + \underline{E}_i. \tag{4}$$

In this manner the strategy is similar to that from the previous section: to determine $\underline{E}(x,y,z)$ from $\underline{E}(x,y,0)$, where z is small.

The basic idea is that $\underline{E}(x,y,z) - \underline{E}_h(x,y,z) = \underline{E}_i(x,y,z)$ is small if z is small. We can write from (1) and (4)

$$\underline{\nabla} \times (\underline{\nabla} \times (\underline{E}_h + \underline{E}_i)) - k_0^2 (\underline{\underline{\varepsilon_B}} + \underline{\underline{\Delta\varepsilon}}(\underline{r}))(\underline{E}_h + \underline{E}_i) = 0, \tag{5}$$

and (2)

$$\underline{\nabla} \times (\underline{\nabla} \times \underline{E}_h) - k_0^2 \underline{\underline{\varepsilon_B}} \underline{E}_h = 0 \tag{2'}$$

Subtracting ((2′)) from (5)

$$\underline{\nabla} \times (\underline{\nabla} \times \underline{E}_i) - k_0^2 (\underline{\underline{\varepsilon_B}} + \underline{\underline{\Delta\varepsilon}}(\underline{r}))\underline{E}_i - k_0^2 \underline{\underline{\Delta\varepsilon}}(\underline{r}) \underline{E}_h = 0. \tag{6}$$

If it is true that

$$\lim_{z \to 0} \underline{E}_i(x,y,z) = 0, \tag{7}$$

and z is infinitesimally small, then (6) can be further simplified

$$\underline{\nabla} \times (\underline{\nabla} \times \underline{E}_i) - k_0^2 \underline{\underline{\varepsilon_B}} \underline{E}_i = k_0^2 \underline{\underline{\Delta\varepsilon}}(\underline{r}) \underline{E}_h. \tag{8}$$

The right side of the equation is known. For simplicity we denote it with a new variable

$$k_0^2 \underline{\underline{\Delta\varepsilon}}(\underline{r}) \underline{E}_h := \underline{M}(\underline{r}).$$

Thus

$$\underline{\nabla} \times (\underline{\nabla} \times \underline{E}_i) - k_0^2 \underline{\underline{\varepsilon_B}} \underline{E}_i = \underline{M}(\underline{r}). \tag{9}$$

Taking the Fourier transform of $M(x,y,0)$:

$\underline{\tilde{M}}(k_x,k_y) = \iint \underline{M}(x,y,0)\exp[-i(k_x x + k_y y)]dx \cdot dy$, similar to the inverse Fourier transform:

$$\underline{M}(x,y,0) = \iint \underline{\tilde{M}}(k_x,k_y)\exp[i(k_x x + k_y y)]dk_x \cdot dk_y/4\pi,$$

we can get for small z:

$$\begin{aligned}\underline{M}(x,y,z)|_{z\text{-small}} = &\iint \begin{bmatrix} \tilde{M}_x \exp(i\delta k_{zx} z) \\ \tilde{M}_y \exp(i\delta k_{zy} z) \\ \tilde{M}_z \exp(i\delta k_{zz} z) \end{bmatrix} \exp(ik_{oz} z) \\ &\cdot \exp[i(k_x x + k_y y)]dk_x \cdot dk_y/4\pi,\end{aligned} \tag{10}$$

which is true for the zeroth and first order (of z) when the wave vector like δk_{zi} parameters are properly chosen. All $\tilde{M}_i$ and δk_{zi} are functions of (k_x,k_y).

Similar to the above procedure, according to the basic idea we search E_i in the following form to solve Eq. (9):

$$\underline{E}_i(\underline{r}) = \iint \underline{\tilde{E}}_i(k_x,k_y,z)\exp[i(k_x x + k_y y)]dk_x \cdot dk_y/4\pi. \tag{11}$$

An important novelty of the model is that we assume the components of $\underline{\tilde{E}}_i(k_x,k_y,z)$ as polynomial functions of z (the legitimacy of this is discussed in the Appendix A)

$$\underline{\tilde{E}}_i(k_x,k_y,z) = \begin{bmatrix} b_x z + a_x z^2 + \dots \\ b_y z + a_y z^2 + \dots \\ b_z z + a_z z^2 + \dots \end{bmatrix} \exp(ik_{oz} z). \tag{12}$$

All a_i-s and b_i-s are also functions of k_x, k_y and k_{oz}.

Using this assumption Eq. (9) is solvable, and we get as solution values for a_i and b_i for each considered (k_x,k_y) pair.

Nevertheless (7) is not generally true. A small constant term c appears in the square brackets in the general case

$$\underline{\tilde{E}}_i(k_x,k_y,z) = \begin{bmatrix} c_x + b_x z + a_x z^2 + \cdots \\ c_y + b_y z + a_y z^2 + \cdots \\ c_z + b_z z + a_z z^2 + \cdots \end{bmatrix} \exp(ik_{oz} z). \tag{13}$$

We found it practical to introduce a new variable

$$\underline{\tilde{E}}_{i,c}(k_x,k_y,z) := \begin{bmatrix} c_x \\ c_y \\ c_z \end{bmatrix} \exp(ik_{oz} z) = \underline{c}\exp(ik_{oz} z).$$

Thus Eq. (8) is modified for $\underline{E}_i$:

$$\underline{\nabla} \times (\underline{\nabla} \times \underline{E}_i) - k_0^2 \underline{\underline{\varepsilon_B}} \underline{E}_i = k_0^2 \underline{\underline{\Delta\varepsilon}}(\underline{r})(\underline{E}_h + \underline{E}_{i,c}). \tag{14}$$

This is an implicit equation which can be solved by iteration in the following way:

$\underline{E}_{i,c} := 0 \Rightarrow$ substituting this into Eq. (14), E_i can be determined. It also contains a term $E_{i,c}$. Repeatedly substituting the new $E_{i,c}$ into Eq. (14), the value of E_i becomes more and more accurate. However, the value of the $E_{i,c}$ is always very small since $\underline{\underline{\Delta\varepsilon}}(\underline{r}) \ll \underline{\underline{\varepsilon_B}}$, so the second step of the iteration is also always sufficient.

In the first iteration step we substitute (10), (11), and (13) into Eq. (14), abandoning the integral (it can be done because of the linearity), and get the following equation:

$$\left(-k_0^2\underline{\varepsilon}_B+\underline{\nabla}\times\underline{\nabla}\times\right)\left(\begin{bmatrix}c_x+b_xz+a_xz^2+\cdots\\ c_y+b_yz+a_yz^2+\cdots\\ c_z+b_zz+a_zz^2+\cdots\end{bmatrix}e^{i(k_xx+k_yy+k_{oz}z)}\right)$$
$$=\begin{bmatrix}\tilde{M}_x\exp(i\delta k_{zx}z)\\ \tilde{M}_y\exp(i\delta k_{zy}z)\\ \tilde{M}_z\exp(i\delta k_{zz}z)\end{bmatrix}e^{i(k_xx+k_yy+k_{oz}z)}, \quad (15)$$

for each (k_x,k_y).

If the equality is solved to zeroth order (in z), then it gives 3 scalar equations (zeroth order solution), if solved to zeroth and first order, then it gives 6 scalar equations (first order solution). It can be shown that the vector c has neither ordinary nor extraordinary projection, which means that it must be perpendicular to them, so the direction of c is determined, only its length is indefinite.

$$\underline{c}(k_x,k_y)=c(k_x,k_y)\cdot\underline{e}_c(k_x,k_y).$$

Consequently in the zeroth order solution we get c, b_x and b_y, and in the first order solution a_x, a_y, b_x, b_y, b_z and c (all coefficients are functions of k_x and k_y).

It can be seen that if the applied distance between the consecutive planes, d, is small enough, the first order solution does not improve the accuracy of the full solution effectively. (Small d is needed for the Eqs. (8) and (14) to remain true.) In this case it is enough if the wave equation is satisfied to zeroth order. Thus b_z and all a_i-s are negligible, they do not increase the convergence.

The described method differs substantially from the well known successive approximation method [4,7,8,10], since it does not only multiply the field distribution in the consecutive planes with a transmission term, but combines the propagation with the inhomogeneous refractive index distribution to form a perturbation, which affects all parameters of the field (phase, amplitude, polarization).

We implemented the above calculation numerically using fast Fourier transform algorithms. After the proper selection of the x, y and z axes, matched to the propagation direction of the incident beams and the optic axis we generate a grid in the x, y plane with the mesh points distanced by s_x and s_y, respectively. For simplicity the x and y axes are chosen parallel and perpendicular to the acoustical plane wave.

The spatial grid determines a reciprocal k_x, k_y grid in the Fourier plane, of the same resolution. We get the c, b_x and b_y parameters for each mesh point in the Fourier plane by (15) and get the E_i field vector values in a next plane distanced by d in z direction by inverse Fourier transformation according to (11). The full field at the grid points is given by (4), where E_h is obtained from (3).

3. Modeling results

3.1. Physical environment

We used the following parameters to test our model (material is TeO_2). We chose ordinary polarized Gaussian beam as input field distribution. The symmetry axes of the optical and acoustic beams lie in the x–z plane, which can be called interaction plane. The z axis is chosen perpendicular to the acoustic beam. To get a real configuration geometry and to fulfill the Bragg condition in a given acoustic frequency range, the incident optical beam must propagate at a certain angle τ relative to the z axis and at a second angle γ relative to the optic axis. In our case the angle γ between the z axis and the optical axis is of 3°. We performed the calculation at different angles τ to find the angle where the highest diffraction efficiency at a given interaction length and acoustic perturbation

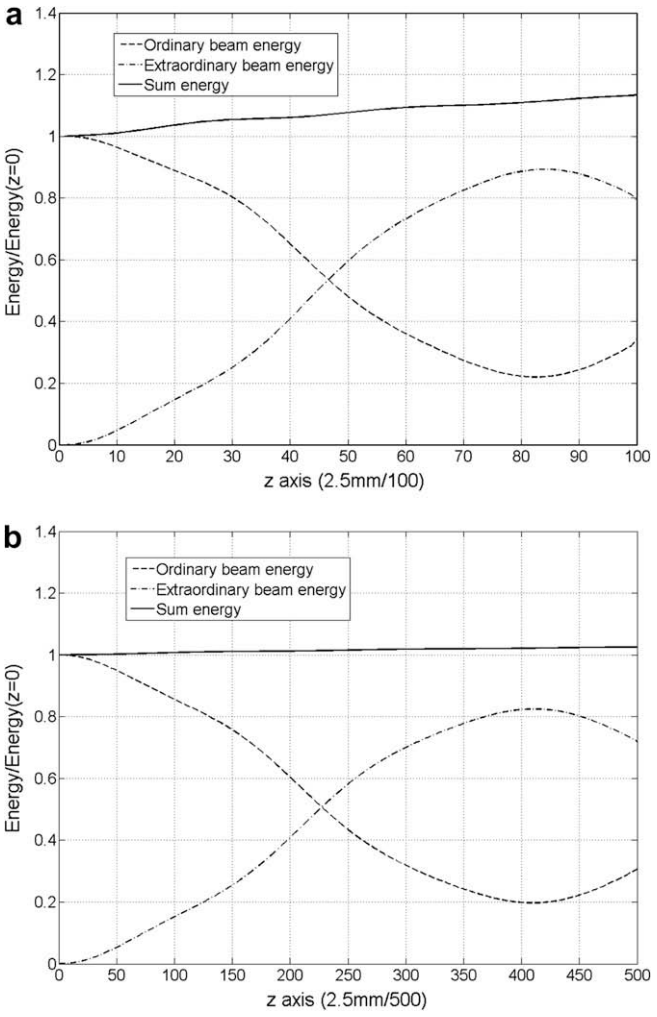

Fig. 1. Evolution of the electromagnetic energy carried by the ordinary beam, extraordinary beam and both along the z axis within an anisotropic acousto-optic interaction governed by the parameters listed in Section 3.1. (a) The resolution along the z axis is 100, (b) the resolution along the z axis is 500.

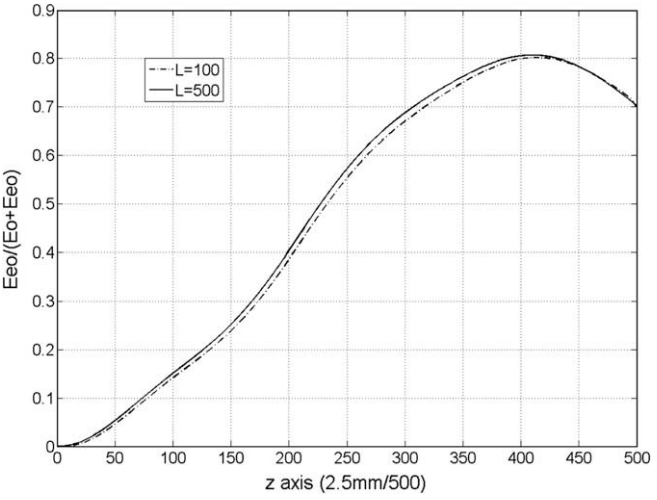

Fig. 2. Evolution of the diffracted beam's energy related to the sum energy along z, compared at resolution 100 and 500 along z.

occurs. For the Figs. 1, 2, 5, 6 and 8 as an input parameter we applied the τ angle of $\sim 0.75^\circ$ (outside the crystal it seems to be $\sim 1.7^\circ$).

Ordinary refractive index:	no = 2.2588,
extraordinary:	ne = 2.4118.

The optical axis lies in the x–z plane, its angle to axis z:

$\gamma = 3^\circ$.

Gaussian beam parameters:

wavelength in vacuum:	λ_0 = 633 nm,
beam waist width:	W_0 = 46.269 μm.

Sizes of the processed volume:

size in x direction:	h_x = 0.8 mm,
size in y direction:	h_y = 0.4 mm,
size in z direction:	h_z = 2.5 mm.

The applied refractive index distribution:

$$\underline{\underline{\Delta\varepsilon}}(\underline{r}) = A \cdot \underline{\underline{\Delta\varepsilon}}_0 \cdot \sin(K \cdot x),$$

where

$$\underline{\underline{\Delta\varepsilon}}_0 = \begin{pmatrix} 0 & 1 & 0 \\ 1 & 0 & 0.007313 \\ 0 & 0.007313 & 0 \end{pmatrix}, \quad A = 6.511^{*}10^{-4},$$

acoustic wavelength:	$2\pi/K$ = 9.0286 μm.
the Klein–Cook parameter:	$Q = h_z K^2/k$ = 54.

3.2. Electromagnetic energy conservation

During the calculation we did not need to set the energy conservation as a condition. Thus energy conservation can be used as a proof of mathematical and physical accuracy.

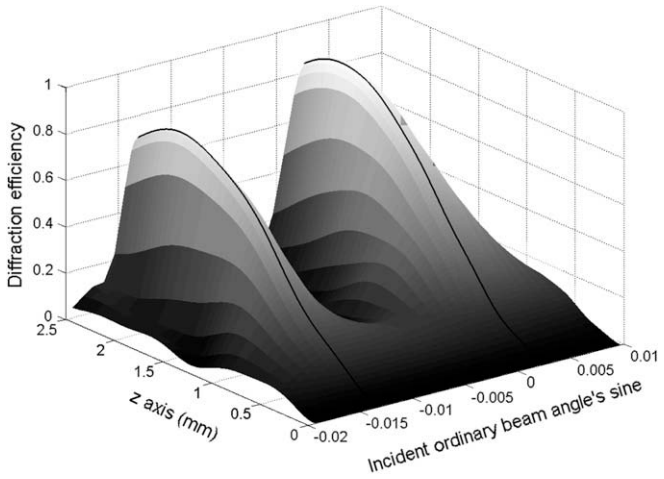

Fig. 3. Dependence of the diffraction efficiency on the incidence angle and z. The function has two maxima indicating two Bragg angles. The black solid curves correspond to the Bragg angles and diffraction efficiencies calculated with analytical formulae derived from the Dixon equations. Note the coincidence between the Bragg angles calculated analytically and with our model.

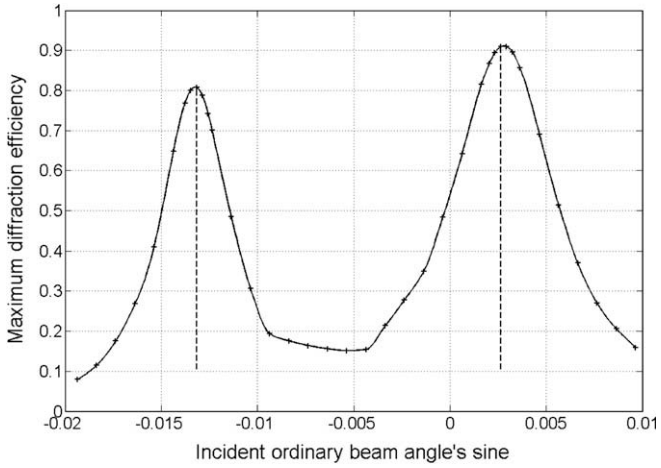

Fig. 4. Dependence of the maximum diffraction efficiency on the incidence angle. The dashed lines denote the Bragg angles calculated with analytical formulae.

One can expect that decreasing step size and increasing resolution increases accuracy and decreases the error. We calculated the energy sum of all diffracted orders in each consecutive processed plane along the z axis and defined the energy error as the difference between this sum and the incident beam's energy. Our main observation was in concordance with the expectations, so that the error in the energy conservation is linearly proportional to the resolution (number of processed planes) along the propagation direction.

In Fig. 1 light propagates through a Δz = 2.5 mm long refractive grid. For optimal performance we set the incident beam's angle τ to the optimal – lets say Bragg angle. In a first case this distance was partitioned into 100 equidistant steps (Fig. 1a). It can be seen that the energy sum of the ordinary and extraordinary beams' energy is not constant with z, but increased altogether by $\sim$13% within the full propagated length (Δz). In Fig. 1b all parameters are the same, except the number of processed planes, which is five times greater, increasing the resolution along z by five times. It is obvious from the figure that in this case the sum energy deviation becomes five times smaller. Note that the required computational time is also five times greater.

Thus we demonstrated the linear relation between energy error and step size along the z axis, namely k times greater resolution results in k times smaller energy error. Other aspects of the diffraction, like electromagnetic field distribution in a given plane and the diffraction efficiency's dependence on τ are not affected drastically by the computational resolution along the z axis.

However, the energy in the different diffracted beams gives directly the diffraction efficiency, as a main output parameter.

Since the energy of the diffracted field can be calculated directly from its electric field distribution and also from the shrinkage of the zero order beam's energy, a question arises that which energy calculation method converges faster (hereby we can simply reduce computational time).

After examining simulations with different parameters we found the following formula as the most rapidly converging expression for the diffracted field's energy:

$$E^{final}_{diffracted}(z) = E_{diffracted}(z) \cdot \frac{\sum E(0)}{\sum E(z)}, \tag{16}$$

where $E^{final}_{diffracted}(z)$ is the energy in the diffracted field at the z coordinate, $E_{diffracted}(z)$ is the diffracted energy calculated from its field distribution, $\Sigma E(0)$ is the incident energy and $\Sigma E(z)$ is the sum energy at z.

In the case when the incident beam is the ordinary and the diffracted is the extraordinary beam and the other diffracted orders do not appear (in Bragg regime) the diffraction efficiency can be written as

$$\eta_e^{final} = \frac{E_e^{calc}}{E_e^{calc} + E_o^{calc}}. \quad (17)$$

where η_e^{final} is the diffraction efficiency, E_e^{calc} and E_o^{calc} are the energies in the extraordinary and ordinary beams, respectively, calculated from their field distributions.

It is visible from Fig. 2 that this expression gives good estimation of the diffraction efficiency and it is almost independent of the number of partitions along the distance Δz.

3.3. Geometrical considerations – Bragg diffraction

To get efficient acousto-optic interaction at high Klein–Cook parameter values a strong geometric condition must be fulfilled commonly called Bragg condition. This geometrical rule imposes the directions and polarizations of the incident beam for which the diffraction efficiency reaches its maximum within the shortest interaction length at a given acoustic power. For birefringent (anisotropic) medium these geometrical constraints are described by the Dixon equations.

One can see that at a given acoustic frequency and propagation direction there are two optical incidence angles that satisfy the Dixon equations. We call these angles Bragg angles, and define them as the angles between the incident optic and acoustic beams, τ.

To verify if the model fulfills the geometrical condition we calculated the dependence of the diffraction efficiency on the angle τ (Fig. 3). The diffraction efficiency curves calculated with the Bragg angles resulting from analytical (geometrical) formulae are marked black. In Fig. 4 we show the dependence of the maximal diffraction efficiency on the incident beam angle's sine. Here the Bragg angles derived from Dixon equations are marked with dashed lines.

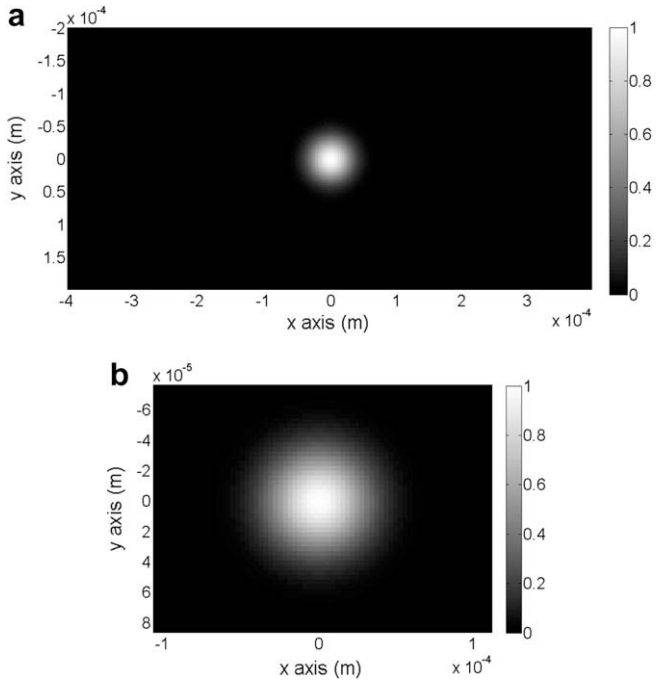

Fig. 5. Spatial intensity distribution of the incident Gaussian beam. (a) Shown on the whole calculation area. (b) Magnified to show the details. Intensity values are represented by the gray scale (arbitrary units).

It is visible that our model gives the maximal diffraction efficiencies exactly at the Bragg angles calculated from the Dixon equations. Thus we have shown that the model satisfies well the geometrical condition.

The calculations were performed on Gaussian beams (Fig. 5a and b) whereas exact Bragg condition can be fulfilled only by plane waves. This fact results in two characteristics: on one hand the theoretical efficiency does not achieve 100% and on the other hand maximum diffraction efficiency dependence on the incidence angle is not a Dirac delta. As we conceive the Gaussian beam as a summation of near parallel plane waves we see that only one plane wave can satisfy the Bragg condition exactly. So the maximal diffraction efficiency occurs when the 'central' plane wave component – of maximum amplitude – fulfills the Bragg condition. The direction of this 'central' plane wave coincides with the propagation axis of the Gaussian beam usually referred to as beam axis.

This behavior can be seen well on the spatial intensity spectrum (absolute square of the Fourier transformed field $(|\tilde{E}_o(k_x, k_y, z)|^2)$), since this function gives the intensities of different plane waves as a function of wave vector coordinates (k_x, k_y). One can see that

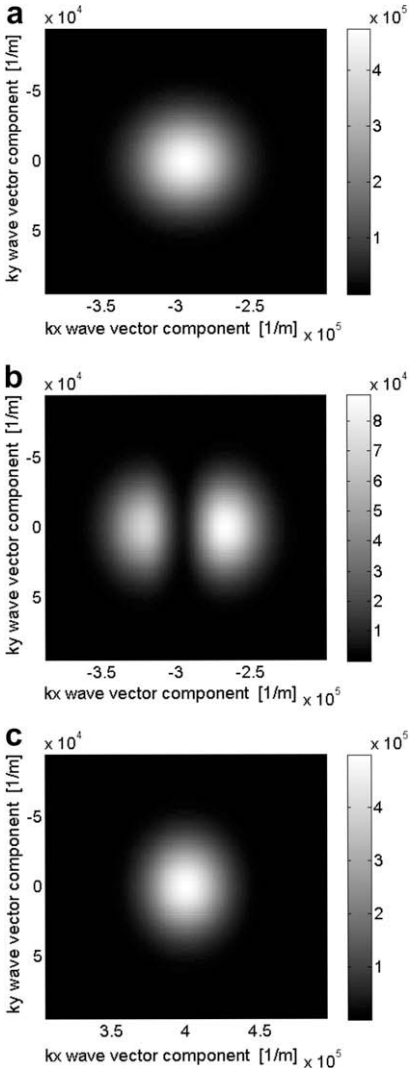

Fig. 6. Zoom of the spatial intensity spectrum of the (a) incident ordinary beam, (b) ordinary (non-diffracted) beam after the acousto-optic interaction in the $z = 2.5$ mm plane. (c) extraordinary (diffracted) beam after the acousto-optic interaction in the $z = 2.5$ mm plane. Intensity values are represented by the gray scale (arbitrary units).

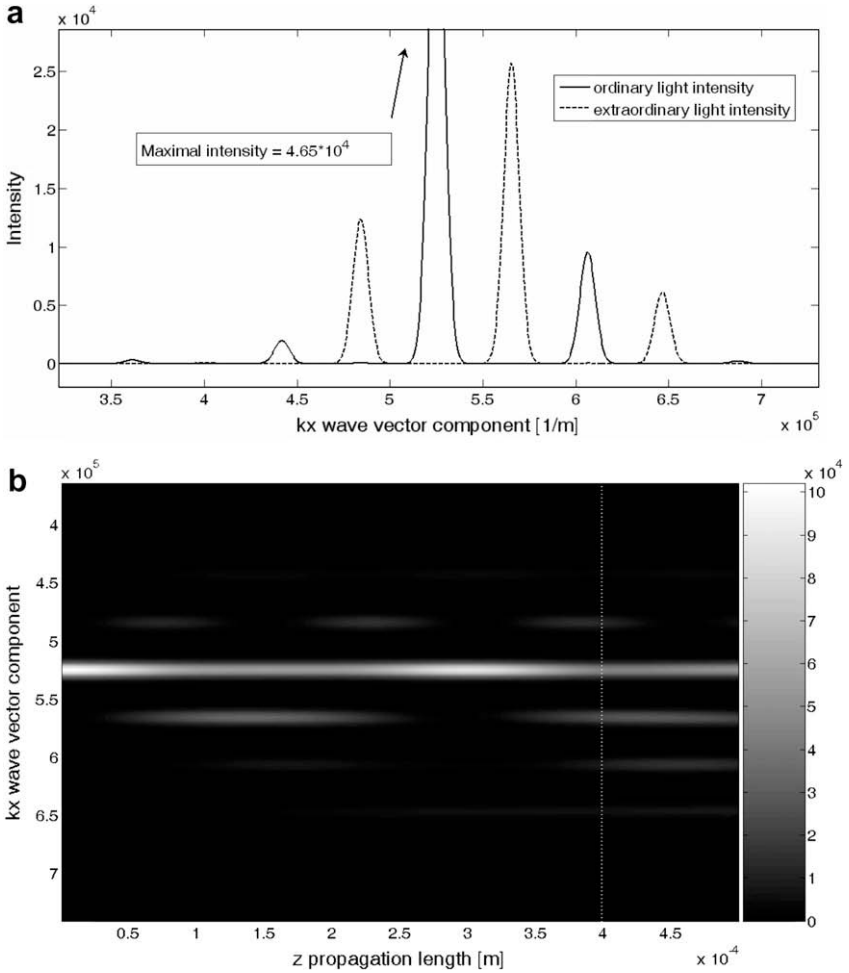

Fig. 7. The intensity spectrum of the propagating light: (a) at the plane of $z = 4$ mm, (b) as a function of z. (The dotted line shows the place of Fig. 7a.) Intensity values are represented by the gray scale (arbitrary units). The Klein–Cook parameter is 100 times smaller than in Fig. 3 and therefore more orders appear in the diffraction.

the Fourier transform of the incident ordinary beam has a shape resembling a two-dimensional normal distribution (Fig. 6a). At the z coordinate where the diffraction efficiency is maximal the center of the spot is depleted and the two sides are less lowered (Fig. 6b). The field lacking from the depleted part of the ordinary beam is transferred to the diffracted extraordinary beam (Fig. 6c).

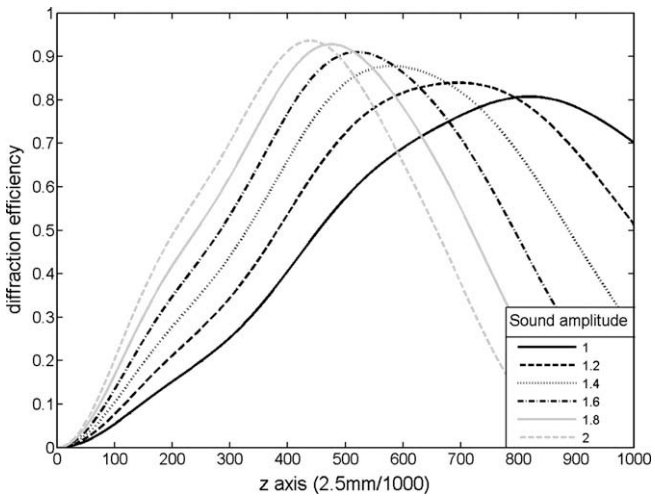

Fig. 8. Dependence of the diffraction efficiency – z curve on the relative sound amplitude.

3.4. Raman-Nath diffraction

In Fig. 7a and b we present a simulation of the field evaluation with 100 times smaller Q parameter ($Q = 0.54$). In this case the interaction is at the limit of the Bragg regime. As expected from previous simulations [4,5,11] more than one diffracted orders appeared – Raman-Nath diffraction. Their amplitudes vary roughly periodically with the propagated distance z. One cross section is presented in Fig. 7a. The intensity spectrum is shown as a function of the k_x wave vector component.

To set these conditions we used the parameters of Section 3.1 except three values: the acoustical wavelength is ten times greater, 90.286 μm (the acoustical frequency and wave vector are ten times smaller). In fact that change would have been already enough however for the visibility we needed smaller pattern in the spectrum. For that we enlarged three times both the incident beam's waist width and the sizes of the volume in x and y directions.

$$Q = LK^2/k = 0.54.$$

3.5. Simulating the efficiency dependence on the acoustical power

Qualitative physical picture of the interaction, resulting also from the previously used mathematical simulations, shows that increasing acoustic amplitude causes faster diffraction evolution along axis z and it is also known that this increases even the diffraction efficiency. The results of the simulation are in complete

agreement with these expectations (Fig. 8). The diffraction efficiency curves are not simple sine functions because the beams are not plane waves but Gaussian.

The parameters of these simulations are the same as in the Section 3.1, the only difference is that the amplitude of the refractive index variance is multiplied with the relative sound amplitude denoted in Fig. 8.

4. Conclusion

In this paper general formalism was shown to calculate the vectorial wave equation (deduced from the Maxwell's equations) with high accuracy, in cases where the medium is inhomogeneous and anisotropic. We provided the detailed mathematical description of the method.

The only utilized assumptions are that the applied light is monochromatic, the reflecting beams are negligible, and the amplitude of the dielectric tensor's spatial variation is relatively small.

These conditions are applicable for the acousto-optic phenomena, for which the model was primarily created.

The presented results of the calculations modeling acousto-optic interaction in uniaxial medium were in concordance with natural physical expectation: electromagnetic energy was conserved, the diffraction efficiency was maximal in directions that fulfill the Bragg condition given by analytic formulae. Qualitatively, the analytic formulae of the Bragg diffraction gave the same results with the same parameters in terms of propagation angle, interaction length and acoustic power. Using smaller Klein–Cook parameter more diffractional orders occur – as it is expected.

Appendix A

In this section we discuss why it is useful to search $\tilde{\underline{E}}_i$ in the form of (12) and (13).

First, every f Fourier transformable function can be written in the form

$$f(x,y,z) = \iint \tilde{f}(k_x,k_y,z)\exp[i(k_x x + k_y y)]\frac{dk_x dk_y}{4\pi^2}$$

(f can be even a vector function, then $\tilde{f}$ is also vector function.) And without loss of generality the components of $\tilde{f}$ can be approximated according to the following expansion into series:

$$\tilde{f}_j(k_x,k_y,z) = [c_j(k_x,k_y) + b_j(k_x,k_y)\cdot z + a_j(k_x,k_y)\cdot z^2 + \cdots] \cdot \exp(ik_{oz}z).$$

To search $\tilde{E}_{ix}$, $\tilde{E}_{iy}$ and $\tilde{E}_{iz}$ in this form is effective for as much as $\tilde{\underline{E}}_i = \tilde{\underline{E}} - \tilde{\underline{E}}_h$, where the k_z wave vector component of $\tilde{\underline{E}}_h$ and $\underline{E}$ can vary between k_{oz} and k_{ez} (usually a small variance). Consequently the same can be said about $\tilde{\underline{E}}_i$. It follows that the polynomial part of the components of $\tilde{E}_i$ varies slowly, by other words, the first part can be well approximated by polynomial. If (7) is fulfilled then the first, the constant part of the polynomial is zero.

References

[1] A. Ciattoni, C. Palma, Opt. Commun. 231 (2004) 79.
[2] A. Ciattoni, B. Crosignanic, P. Di Porto, Opt. Commun. 202 (2002) 17.
[3] G. Zhou, K. Zhu, F. Liu, Opt. Commun. 276 (2007) 37.
[4] A. Korpel (Ed.), Selected Papers on Acousto-optics, vol. MS16 of SPIE Milestone Series, 1990.
[5] J. Xu, R. Stroud, Acousto-Optics, Wiley, NY, 1992.
[6] P. Maák, T. Takács, A. Barócsi, E. Kollár, V. Székely, P. Richter, Opt. Commun. 266 (2006) 419.
[7] C. Venzke et al., Appl. Opt. 31 (1992) 656.
[8] C.W. Tarn, R.S. Huang, J. Opt. Soc. Am. A 14 (1997).
[9] R. Huang, C.W. Tarn, P. Banerjee, Opt. Eng. 38 (1999) 1122.
[10] I. Grulkowski, P. Kwiek, Eur. Phys. J. Spec. Top. 154 (2008) 77.
[11] F.W. Windels, O. Leroy, J. Opt. A: Pure Appl. Opt. 3 (2001) S12.
[12] L. Adamowicz, Van Q. Nguyen, Opt. Laser. Eng. 35 (2001) 67.
[13] G. Zhou, Opt. Laser Technol. (2008), doi:10.1016/j.optlastec.2008.01.003.
[14] A. Ciattoni, P. Di Porto, B. Crosignani, A. Yariv, JOSA B 17 (2000) 809.
[15] O.J.F. Martin, N.B. Piller, Phys. Rev. E 58 (1998) 3909.
[16] O.J.F. Martin, Int. J. Electron. Commun. (AEU) 58 (2004) 93.